

(23) ANALYTICAL STUDY ON THE EFFECT OF CARBON FIBER SHEET ORIENTATION AND CONFIGURATION ON SEISMIC RETROFITTING OF CIRCULAR STEEL COLUMNS UNDER CYCLIC LOADING

Juliane Therese R. BACOD¹ and Hitoshi NAKAMURA²

¹Member of JSCE, Student, Graduate School of Urban Environmental Sciences, Tokyo Metropolitan University
(1-1 Minami-Osawa, Hachioji, Tokyo 192-0397, Japan)
E-mail: bacod-juliane-therese-rellas@ed.tmu.ac.jp

²Member of JSCE, Associate Professor, Graduate School of Urban Environmental Sciences, Tokyo Metropolitan University
(1-1 Minami-Osawa, Hachioji, Tokyo 192-0397, Japan)
E-mail: hnaka@tmu.ac.jp

This study investigated the effect of carbon fiber (CF) sheet orientation and configuration on the retrofitting performance of externally bonded CF sheets on circular steel columns subjected to cyclic lateral loads. A parametric study using finite element analysis (FEA) was conducted to determine the optimal combination of CF sheet orientations and configurations for a proposed retrofit design method. The corresponding column behavior was monitored for each variation of the CF sheet fiber direction with respect to the horizontal and the combination of uniform and graded CF sheet arrangements. The proposed retrofit design method intends to address the stress concentrations and buckling deformations near the base of the column while minimizing the inward buckling due to the high constraining effect of the CF sheets. This study considers a reinforcement case, R, wherein CF sheets are applied before loading. The results showed that the proposed reinforcement model can effectively increase the horizontal load-displacement capacity, and energy absorption capacity of the retrofitted column. Outward buckling deformations are suppressed without causing significant inward buckling that contributes to the sudden decrease in the column's load carrying capacity at larger displacement cycles. An experimental study is intended to be conducted in the future to further verify the results of this analytical study.

Key Words: carbon fiber sheet, circular steel bridge pier, seismic retrofitting, buckling, finite element analysis

1. INTRODUCTION

Circular steel columns are identified to be susceptible to local buckling or even rupture due to excessive inelastic deformations when subjected to strong lateral loads. In the case of the damages observed after the Kobe Earthquake in 1995, buckling damages were found at various parts of the columns such as the base (elephant foot buckling), third point along the column height, and near structural discontinuity (or stiffness changes)¹. Therefore, an effective seismic retrofitting measure shall be implemented to mitigate these issues that can lead to structure collapse. Carbon fiber (CF) sheet wrapping is one of the well-known seismic retrofitting techniques for steel bridge piers utilized to suppress local buckling and delay the

onset of plastic deformation.

In existing experimental studies, it was shown that CF sheet wrapping in the circumferential direction indeed suppresses outward buckling; however, its high constraining effect eventually causes inward buckling which leads to a sudden drop in the horizontal capacity². On the other hand, CF sheet wrapping in the longitudinal direction provides a better increase in the horizontal load capacity but debonding was more evident at the end of the loading cycle³. To potentially address these concerns and optimize the strength of each wrapping direction, investigation of the effect of the CF sheet orientation on the effectiveness of a retrofitting design can be a good consideration.

In this study, a parametric study using finite element modeling and analysis was conducted to investigate the effect of CF sheet orientation, number of layers, and configuration on the overall behavior of retrofitted circular steel column. The reinforcement effect of the CF sheet design method was evaluated in terms of the resulting horizontal load-displacement capacity, energy absorption capacity, and buckling modes. This study ultimately aims to propose an effective CF sheet reinforcement design method to lessen the probable inward buckling, improve performance and buckling modes, and to reduce stress and damage concentrations on column discontinuities.

2. SPECIMEN DESIGN AND TEST SET-UP

(1) Circular Steel Column

The circular steel column specimen considered in this analytical study is a JIS STK400 standard column section as shown in Fig. 1 with properties shown in Table 1. The column has thicker sections and stiffening ribs at the lower regions to prevent local buckling near the base. Base anchorage of the columns is composed of 12-M36 bolts tightened using hydraulic bolt tensioning with final pre-tensioning equal to 50 MPa. This base column specimen denoted as the unreinforced case (N) serves as the benchmark and control set up at which the results from the parametric study for the retrofitting cases were evaluated. This study considers a reinforcement case, R, wherein CF sheets are applied before loading.

(2) Loading Program

In the vertical direction, the column was subjected to a constant axial load equal to 10% of the yield axial force to approximate the superstructure weight. In the horizontal direction, the column was subjected to an increasing cyclic lateral load by displacement control. The lateral load is composed of increasing increments of the calculated horizontal yield displacement of the column specimen (δ_y) equal to 10 mm. A maximum displacement load of $\pm 12\delta_y$ was applied in the analysis to determine the column's behavior at higher load displacement cycles beyond the failure point. The failure point is defined as the displacement at which the maximum horizontal load capacity post-peak drops to 5% of the maximum and is used as the measure of the column's ductility.

The lateral displacement loading program in Fig. 2 was implemented in the analysis of the unreinforced (N) and reinforcement (R) analysis cases.

(3) Carbon Fiber Sheet Properties

Unidirectional high strength CF sheets (UT70-30G) were utilized as the retrofitting material. It is

intended to be bonded to the steel column specimen using AUP40 epoxy resin via vacuum-assisted resin transfer molding (VaRTM). This method of impregnating CF sheet layers with resin produces the carbon fiber reinforced polymer (CFRP). The CF sheet retrofitting in the modeling and analysis was executed using the properties of the CFRP. Table 1 summarizes the properties of the CF sheets, epoxy resin, and resulting CFRP.

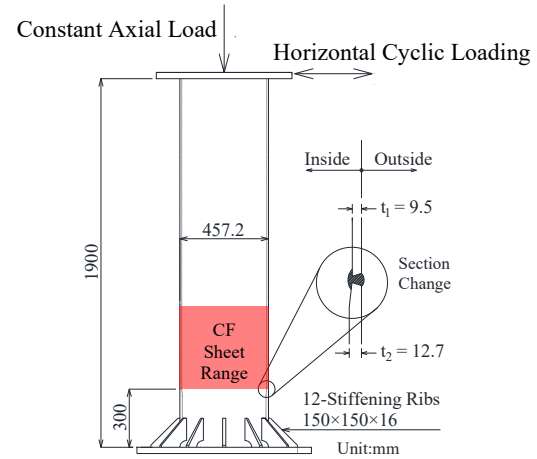


Fig.1 Schematic Diagram of the Steel Column Specimen

Table 1 Material Properties

Material	Properties	Symbols	Values	Units
Steel (JIS STK400)	Elastic modulus	E	190,200	MPa
	Yield stress	σ_y	363	MPa
Carbon Fiber Sheet (UT70-30G)	Elastic modulus (0°)	E_{cfl}	245,000	MPa
	Tensile strength (0°)	$\sigma_{f, t}$	3400	MPa
	Poisson's ratio (0°)	ν_{cfl}	0.2	-
	Design thickness	t_{cf}	0.167	mm
Epoxy Resin (AUP40)	Elastic modulus	E_m	3,430	MPa
	Poisson's ratio	ν_m	0.39	-
CFRP	Fiber content	V_f	50	%
	Thickness (10-layer)	$t_{cfrp, 10}$	0.334	mm
	Thickness (4-layer)	$t_{cfrp, 4}$	0.134	mm
	Longitudinal Elastic modulus	E_1	111,800	MPa
		E_{1ub}	124,200	MPa
		E_{1tb}	6,800	MPa
	Transverse Elastic modulus	E_2	12,900	MPa
		E_{2ub}	7,800	MPa
E_{2tb}		5,400	MPa	
Shear modulus	G_{12}	3,600	MPa	
Poisson's ratio	ν_{12}	0.29	-	

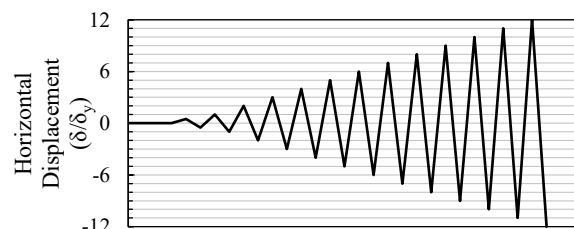


Fig.2 Loading Program

3. ANALYTICAL MODEL AND ANALYSIS METHOD

This study primarily utilized finite element analysis (FEA) to determine the optimal CF sheet reinforcement design. This section summarizes the FEA modeling assumptions and analysis methods implemented in the study. Results from this analytical model assumptions were verified using an existing experimental study⁴⁾.

FEA was performed using the large strain nonlinear analysis procedure of the general-purpose finite element program MSC/Marc Mentat 2019. Updated Lagrange, Additive decomposition procedure was employed to account for geometric nonlinearities. Moreover, multi-stage radial return mapping method was implemented for the calculation of stress states during cyclic elasto-plastic behavior at large strain deformations^{5,6)}.

Lower regions of the model up to 300 mm above the reinforcement area were modeled using 10 x 20 mm mesh size to accurately capture buckling deformations and stress concentrations. The remaining upper regions are modeled with 20 x 20 mm mesh size for practical purposes.

The base plate and bolt assembly are explicitly modeled to account for the induced moments and displacements at the base as observed in the experiments. The circular base plate was modeled using thick shell elements with a touching contact condition with the ground element. Overclosure tying constraints were used to simulate the bolt pre-tension force by applying loads to a control node connected to parts of the bolt element⁷⁾.

Steel elements were modeled using 4-node thick shell elements. On the other hand, the CFRP was modeled using 4-node thin shell elements, as the classical stress-strain relations for this element is similar to that of a unidirectionally reinforced lamina⁸⁾.

The steel material was modeled using an isotropic elasto-plastic material considering von Mises yield criteria and the kinematic hardening law of plasticity. These simplified models are known to predict the cyclic loading behavior of an element with relatively good accuracy. Input values for steel plasticity are based on uniaxial results from coupon tests.

The properties of the CFRP are calculated using the Halpin-Tsai approximate equations with consideration of the upper and lower bound moduli^{9,10)}. The CFRP was modeled using orthotropic material with defined limits to account for the calculated tensile and compressive capacity of the CFRP.

Fig.3 illustrates part of the finite element model constructed in MSC Marc/Mentat 2019.

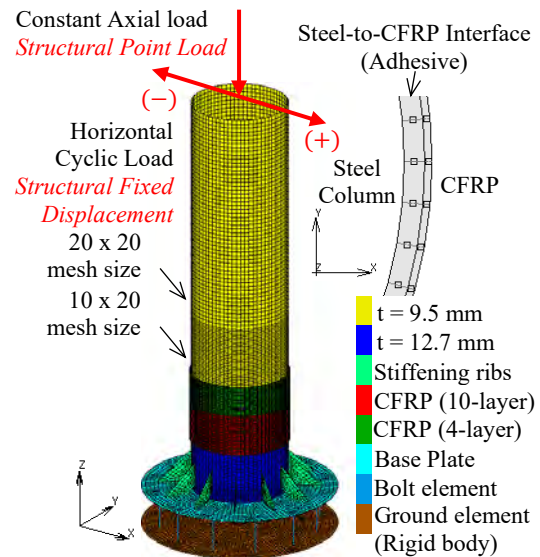


Fig.3 Finite Element Model

4. CF SHEET RETROFITTING DESIGN USING FEA

The proposed CF sheet retrofitting designs were determined from a series of parametric studies by varying the CF sheet orientation, number of layers, and configuration.

First, the CF sheet reinforcement range was established considering the results from the analysis of the unreinforced (N) case. Then, a parametric study was conducted to investigate the effect of CF sheet orientation on varying number of CF sheet layers (CFRP thickness). This primarily aims to investigate the effect of CFRP component stiffnesses to the overall behavior of the column. Optimization of CF sheet configuration was performed based on the distribution of stresses and buckling locations on the columns. The primary objective is to propose a design with high energy absorption capacity and minimize the inward buckling that causes the sudden drop in horizontal load capacity.

(1) Carbon Fiber Sheet Range

The CF sheet reinforcement range was determined based on the resulting buckling modes and stress distribution from the N case. **Fig.4** illustrates the buckling and steel yielding locations on the negative loading side of the N case at $-6\delta_y$ cycle. At failure point, outward buckling occurs from 350 to 450 mm from the column base which accordingly corresponds to the locations of steel yielding along the column height.

With this, the CF sheet wrapping was done over a constant range of 300 mm as shown in **Fig.5**. This is

to primarily address the local buckling and to anticipate the potential redistribution of stresses adjacent to the original failure locations upon the application of the CF sheets. Uniform CF sheet configuration was initially considered on this part of the parametric study.

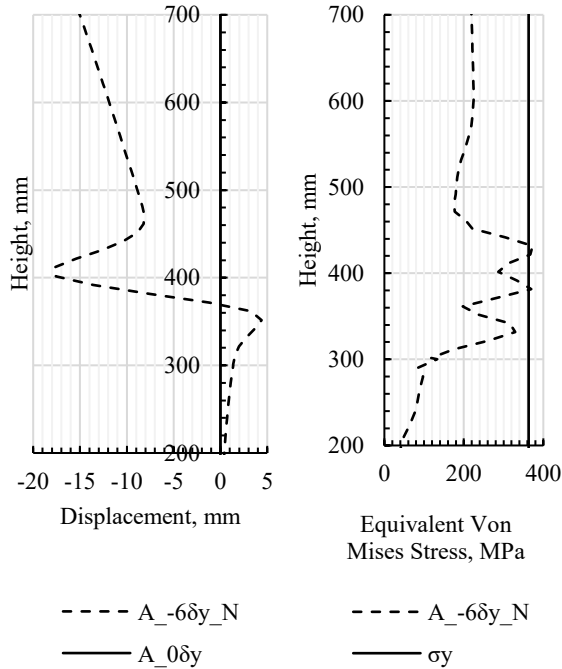


Fig.4 N case buckling location and yield stress distribution at failure.

(2) CF Sheet Orientation

In the analysis, the CF sheet orientation (CFRP fiber direction) is inclined at various angles from the horizontal as shown in **Fig.5**. For consistency and further comparison, CFRP component stiffness for each orientation is resolved on its components in the typical circumferential (x) and longitudinal (y) wrapping directions as summarized in **Table 2**. The primary aim is to characterize the retrofitting effect from the additional CFRP stiffness that the respective orientation provides for each direction.

Furthermore, as has already been established in previous studies, the number of CF sheet layers has a significant effect on the resulting horizontal load capacity and ductility of the reinforced columns. Hence, in this study, the effect of varying CF sheet orientations was investigated along with the number of CF sheet layers, *n*. **Fig.6** shows the relationship between the orientation and stiffness x- and y-components for each case of CF sheet layers. This aids in visualizing the trend between the additional x- and y-component stiffness provided by each orientation wherein at 45° orientation, values of CFRP stiffness components approaches each other and tends to have larger differences as the angle of orientation approaches 0° and 90°.

a) Horizontal load capacity and energy absorption

In this section, the retrofitting effect of the combination of orientation and number of CF sheet layers was investigated considering the resulting energy absorption capacity, and horizontal load capacity at peak and at the end of loading. Each of these parameters are plotted against the fiber orientation for each CF sheet layer model as shown in **Fig.7**.

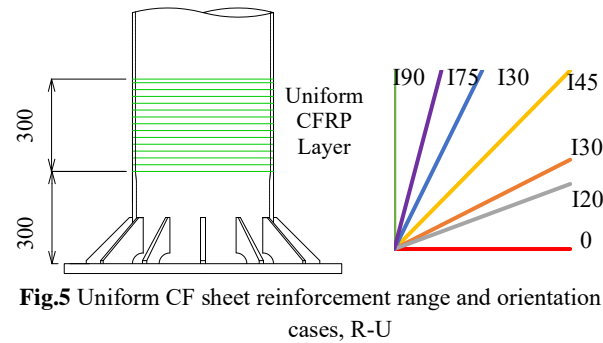


Fig.5 Uniform CF sheet reinforcement range and orientation cases, R-U

Table 2 CF sheet orientation and CFRP stiffness components

CF Sheet Orientation	Angle from horizontal, (°)	$E_{CFRP, X}$	$E_{CFRP, Y}$	$E_{CFRP, X} / E_{CFRP, Y}$ ratio
		N/mm ² x-comp.	N/mm ² y-comp.	
1-layer CFRP stiffness				
0	0	111,800	7,800	0.07
120	20	102,390	45,567	0.45
130	30	92,922	62,655	0.67
145	45	73,539	84,570	1.15
160	60	49,145	100,722	2.05
175	75	21,402	110,009	5.14
190	90	7,800	111,800	14.33

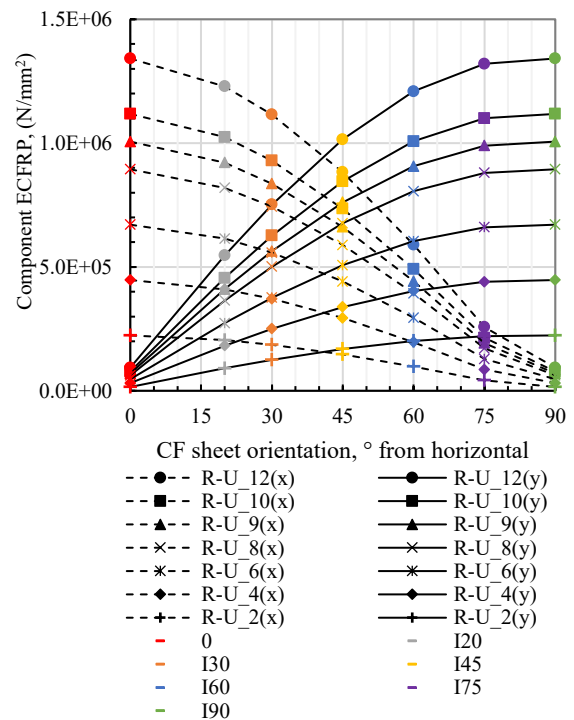


Fig.6 Stiffness components for CF sheet layers and orientation cases (model designations are denoted by R-U_n)

Cases with CF sheet layers ranging from 8 to 12 provided at least a 10% increase in the maximum horizontal load capacity (H_{max}) for all orientation cases. From **Fig.7**, it is evident that providing significantly higher CFRP stiffness on one direction relative to the other, i.e., 0° and 90° orientations, yields higher H_{max} values with up to 20% increase in capacity. However, upon examining the plot for the energy absorption capacity, cases with CF sheets oriented at 0° and 90° yield lower values of energy absorption capacity compared to inclined orientations with x/y component stiffness ratios between 0.45 to 2.05 (20° to 60° orientations). Almost the same trend is noted from the results for the horizontal load capacity at the end of loading at $12\delta_y$ ($H_{12\delta_y}$). Furthermore, relatively higher capacities are clearly observed for 30° and 45° orientations.

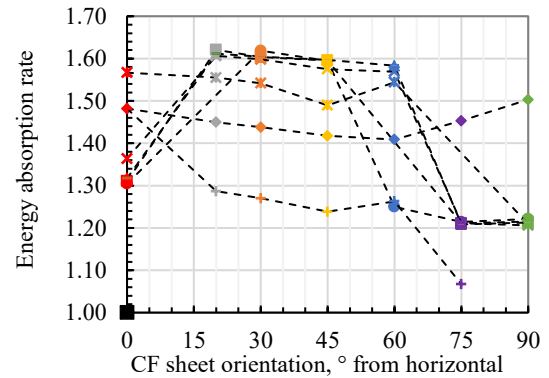
From these set of results, it can be inferred that inclined application of CF sheets on circular steel columns can be beneficial in terms of the resulting energy absorption capacity and increase ductility at higher loading cycles. This can be attributed to readily addressing the anticipated nature of stress distribution across the steel material by allotting adequate amount of additional stiffness on both major stress directions.

From the plots in **Fig.7**, parametric values of CF sheet layers equal to 8 to 12 and orientation equal to 30° and 45° appear to have minimal differences. In order to decide on which of these models to adopt for the succeeding parametric studies, the ductility factors (δ_{95}/δ_y) for each model are further examined and summarized in **Table 3**. The ductility factor corresponds to the failure point of the elements defined by displacement at which the horizontal load capacity drops to 95% of the maximum post-peak. Hence, higher ductility factor corresponds to delayed onset of failure and better performance.

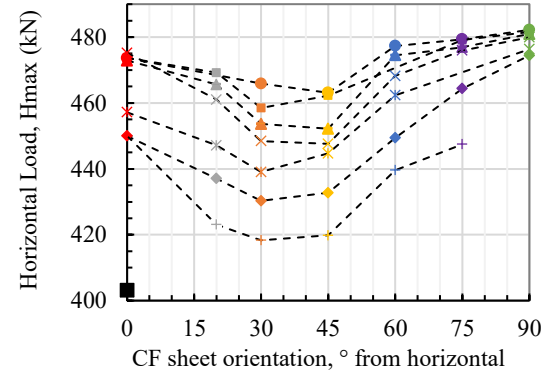
From the summarized data, it can be determined that for a lower CFRP volume, cases with 9 CF sheet layers (R-U_9) approach the same ductility performance as that of cases with 10 (R-U_10) and 12 (R-U_12) CF sheet layers. And although cases with 8 CF sheet layers (R-U_8) approach the energy absorption capacity of models with higher CFRP volumes, it yielded lower ductility factors compared to R-U_9 cases. Hence, R-U_9 models were adopted for the succeeding parametric studies.

b) Horizontal load-displacement curves and buckling deformation

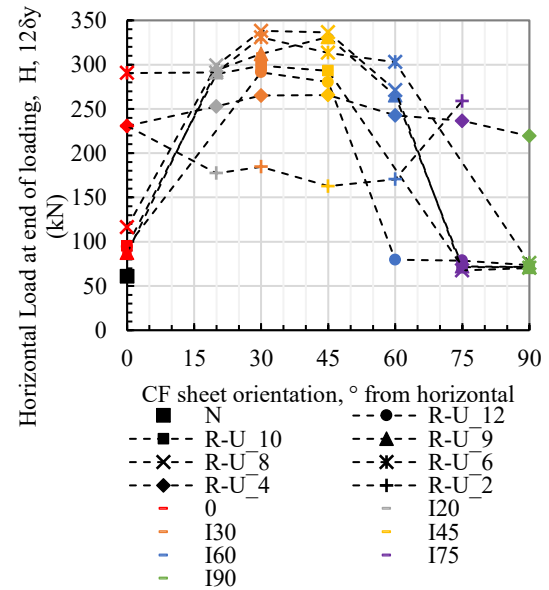
To further visualize the effect of CF sheet orientation on the overall behavior of the reinforced steel column, **Fig.8** and **Fig.9** show the buckling modes at $-6\delta_y$ and envelope curves generated for each orientation case of R-U_9 models.



(a) Energy absorption rate



(b) Maximum horizontal load capacity



(c) Horizontal load capacity at the end of loading

Fig.7 Plots for energy absorption capacity and horizontal load capacity with respect to CF sheet orientation

Table 3 Summary of Ductility Factors

Model	(+ direction)		(- direction)		V_{CFRP} , m^3
	δ_{95}/δ_y	ratio	δ_{95}/δ_y	ratio	
N	4.3	1.00	3.8	1.00	-
R-U 12 I30	8.8	2.05	8.4	2.21	1.74
R-U 12 I45	8.2	1.91	8.1	2.13	
R-U 10 I30	8.3	1.93	8.3	2.18	1.45
R-U 10 I45	7.4	1.72	8.0	2.11	
R-U 9 I30	8.3	1.93	8.5	2.24	1.30
R-U 9 I45	7.5	1.74	7.4	1.95	
R-U 8 I30	7.9	1.84	8.4	2.21	1.16
R-U 8 I45	7.3	1.70	6.8	1.79	

Consistent with the observed trend in the energy absorption capacity, models with CF sheets inclined between 20° to 60° resulted to a more ductile behavior as can be observed from the wider envelope curves.

On the other hand, models with CF sheet inclined near the horizontal and vertical axes resulted in a sudden drop in capacity after peak and lower load capacity at higher loading cycles. This behavior can be further attributed to the resulting buckling modes shown in Fig.9.

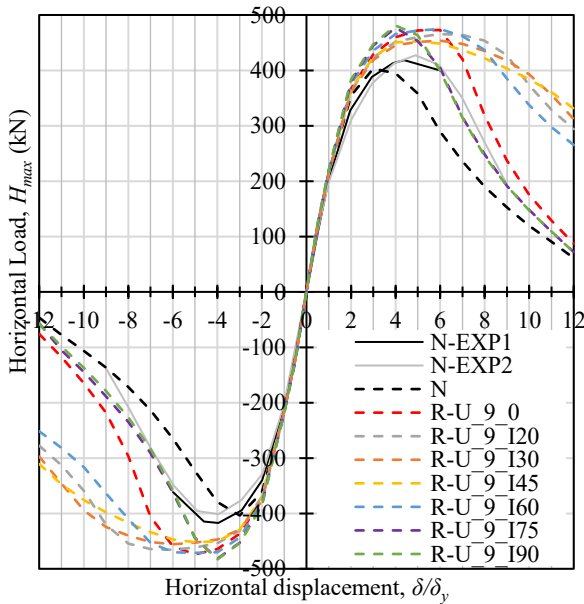


Fig 8. Envelope curves for R-U_9 cases

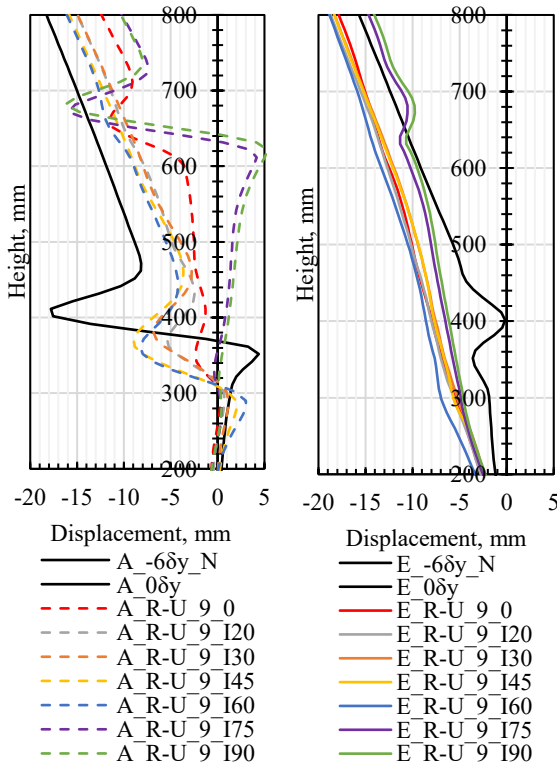


Fig 9. Buckling modes and deformations for R-U_9 cases

All models were able to suppress the previously observed outward buckling from the N case within the 300 mm range of reinforcement. However, models with CF sheet orientation equal to 0°, 75°, and 90° resulted in outward buckling outside the reinforcement range towards the upper portions of the column. This can be attributed to the potential over-reinforcement in one direction and lack of stiffness in the other which led to the redistribution of stresses at the steel level. The unbalanced increase in stiffness in the stress directions led to a shift on the critical stress and buckling location of the column. This behavior eventually caused the yielding of the steel on the weaker areas of the column section.

(3) Carbon Fiber Sheet Configuration

a) Design of Graded Configuration

Recalling the stress distribution from the N case shown in Fig.4, it can be observed that the range from 450 mm to 600 mm from the column base experienced less amount of stress compared to the lower regions where outward buckling occurs. With the aim of optimizing the CF sheet design to be more economical, a graded configuration as shown in Fig.10 was considered. It is composed of 9 layers across the 150 mm range for Segment I covering the entire buckling length observed at lower regions in the analysis and target thin layer CFRP for Segment II for the succeeding 150 mm range. This target thin CFRP region is the subject of this section.

Analysis was conducted for 4- and 6-layer iterations of Segment II for the 30° and 45° orientation cases. R-G_9/6 and R-G_9/4 results to 17% and 24% reduction in CFRP reinforcement ratio, respectively. Reduction was made at these levels to assess if the same level of performance can be achieved with less CFRP volume. The properties of the models considered in the analysis are summarized in Table 4.

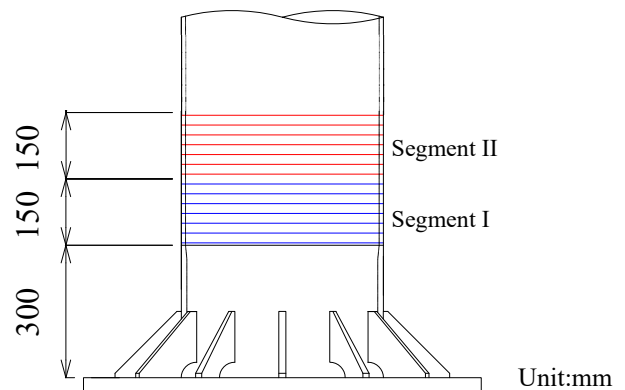


Fig.10. Graded CF sheet configuration

Table 4 Summary of Models for CF sheet configuration

Model	CF Sheet Orientation	Config. type	CF Sheet Layers		Reinforcement Ratio
			I	II	
R-U 9 I30	I30	Uniform	9		1.00
R-U 9 I45	I45	Uniform	9		1.00
R-G 9/4 I30	I30	Graded	9	4	0.72
R-G 9/6 I30	I30	Graded	9	6	0.83
R-G 9/4 I45	I45	Graded	9	4	0.72
R-G 9/6 I45	I45	Graded	9	6	0.83

b) Horizontal load-displacement curve and buckling deformation

The envelope curves and buckling deformations for the considered uniform and graded configurations are shown in **Fig.11** and **Fig.12**. **Fig.12** includes buckling deformations at -9 to provide an overview of the expected column behavior at larger displacement cycles.

The results show that uniform and graded configuration for both orientation cases have minimal differences with respect to the energy absorption capacity characterized by the envelope curves in **Fig.11**. Furthermore, the graded configuration is also as effective as the uniform configuration in suppressing the outward buckling as shown in **Fig.12**. However, there is an observed tendency for inward buckling between 200 mm and 300 mm from the base of the column which coincides with the location of the thickness change of the steel column section. This can be identified as a new potential critical/weak point of the column that needs to be addressed.

Upon taking a closer look at the results for each case, it can be observed that the envelope curve for R-G_9/4_I30 had a faster drop in capacity at the negative loading side compared to other models. This can be related to inward buckling observed at $-6\delta_y$ that evidently progressed at higher loading cycles as shown by the plot with red broken line for $-9\delta_y$ in **Fig.12**. Examining the buckling deformation of R-G_9/6_I30, it also appears to have susceptibility for inward buckling. This progress of inward buckling can be attributed to the relatively higher restraint provided by 30° orientation cases in the circumferential direction compared to that of the 45° orientation cases.

On the other hand, I45 cases provided more stable buckling modes with approximately 2 mm decrease in buckling deformation for the R-G_9/4_I45 compared to the uniform configuration. The minimal change in the level of performance between the uniform and graded configuration for I45 models is also evident from the ductility factors summarized in **Table 5**.

From these results, it can be established that a graded configuration of CF sheets with lower CFRP volume can be as effective as the thicker uniform

configuration provided that the adhesion range, CF sheet layers and orientation are adequately accounted for based on the buckling length and stress distribution across the column height.

Finally, due to the close load-displacement behavior among the models, R-G_9/4_I45 model that has the lower reinforcement ratio and lesser tendency for inward buckling at higher portions of the column was selected as the CF sheet reinforcement design for this study.

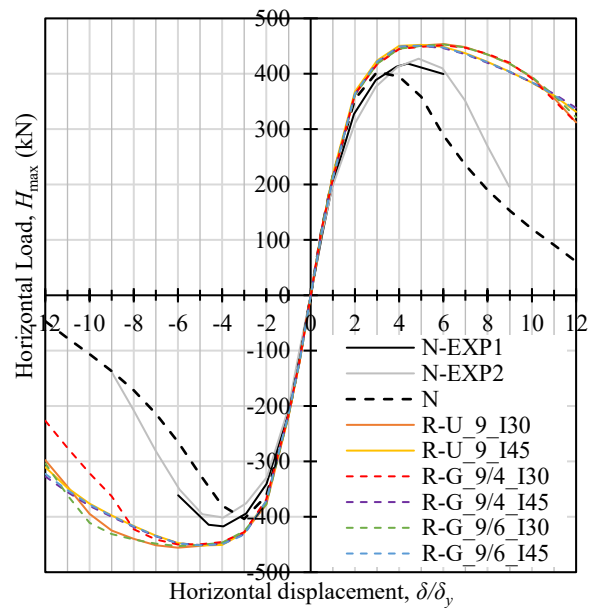


Fig 11. Envelope curves for R-U_9 and R-G_9 cases

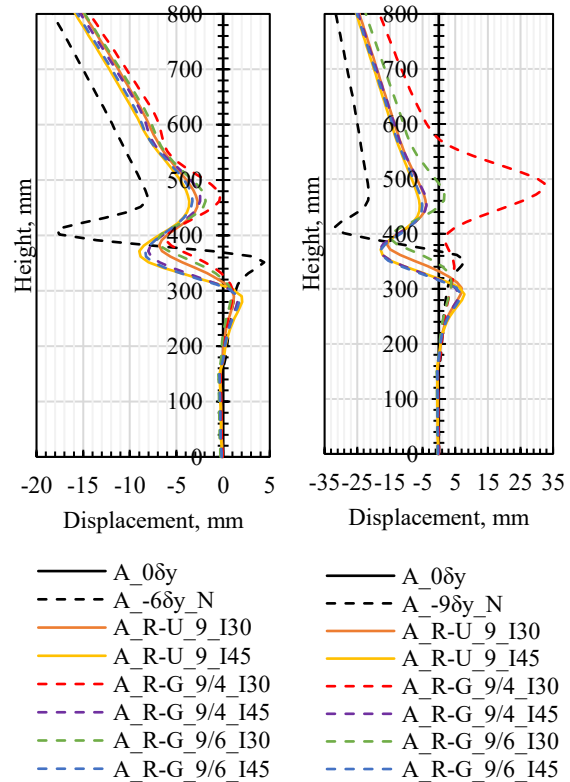


Fig 12. Buckling deformation at $-6\delta_y$ and $-9\delta_y$

Table 5 Summary of Ductility factors

Model	(+ direction)		(-) direction	
	δ_{95}	ratio	δ_{95}	ratio
N	4.3	-	3.8	-
R-U 9 I30	8.3	1.93	8.5	2.24
R-G 9/4 I30	8.4	1.95	7.7	1.79
R-G 9/6 I30	8.3	1.93	9.0	2.09
R-U 9 I45	7.5	1.74	7.4	1.72
R-G 9/4 I45	7.5	1.74	7.4	1.72
R-G 9/6 I45	7.5	1.74	7.3	1.70

5. CONCLUSIONS

In this study, the influence of carbon fiber sheet orientation and configuration was investigated to propose an effective seismic retrofitting design method for circular steel columns. Parametric studies using FEA were conducted to examine the effect of the CF sheet orientation, adhesion range, number of layers, and configuration on the horizontal load-displacement behavior, energy absorption capacity, and buckling behavior of the retrofitted circular steel column. The results obtained from the analysis are summarized below:

1. Inclined CF sheet orientation can improve the circular steel column performance primarily in terms of increased ductility and energy absorption capacity. It was able to suppress outward buckling without causing inward buckling at the upper portions of the column due to stress distribution.
2. Orientations with CFRP x/y component stiffness ratios ranging from 0.45 to 2.05 yielded significantly higher energy absorption capacities compared to orientations that are inclined nearer the typical circumferential (x) and longitudinal (y) wrapping directions.
3. It was observed that a smaller difference between the additional stiffness provided in each stress direction limits the unbalanced increase in stiffness in the stress directions. This unbalance increase in stiffness can cause a shift on the critical stress and buckling location of the column as observed from models with CF sheets oriented at 0° and 90° from the horizontal.
4. Among all cases considered, models with 45° CF sheet orientation provided more stable buckling modes. It also yielded consistent behavior across all thickness and configuration cases in terms of ductility defined by the horizontal load-displacement curves and energy absorption rates.
5. Graded CF sheet configuration with 17% to 24% less CFRP volume can achieve the same level of performance as the uniform configuration provided that the target buckling length and stress

distribution across the column height are adequately accounted for in the reinforcement design.

For future works, improved performance can be targeted by considering an updated graded configuration with same volume as the uniform reinforcement. Extension of the CF sheet adhesion range can be considered to address the inward buckling tendencies near the structural discontinuities of the column. The use of inclined CF sheet orientations can also be considered for its repair effect on the performance recovery of initially damaged circular steel columns.

Lastly, an experimental study is intended to be conducted in the future to further verify the results of this analytical study.

REFERENCES

- 1) Bruneau, M. (1998). Performance of steel bridges during the 1995 Hyogoken-Nanbu (Kobe, Japan) earthquake—a North American perspective. *Engineering Structures*, 20(12), 1063–1078. [https://doi.org/10.1016/S0141-0296\(97\)00203-4](https://doi.org/10.1016/S0141-0296(97)00203-4)
- 2) Okazaki N, Nakamura H, Kishi K, Matsui T, & Setouchi H. (2017). Study on performance recovery of buckling damaged circular steel piers by rolling up carbon fiber sheet. *Journal of Japan Society of Civil Engineers A1 (Structure and Earthquake Engineering)* 73(1), 69-83 [in Japanese] <https://doi.org/10.1016/j.finel.2021.103531>.
- 3) Watanabe, T., Ishida, K., Hayashi, K., Yamaguchi, K., and Ikeda, S. : Seismic Retrofitting of Steel Piers with Carbon Fiber Sheets, *Journal of Structural Engineering*, Vol. 48A, pp. 725-734, 2002.3. (in Japanese)
- 4) Magtagñob, K., Nakamura, H., & Matsui, T. (2021). Effect of Graded Carbon Fiber Sheet Configuration on the Seismic Retrofitting of Circular Steel Bridge Piers, *Proceedings of the 14th Symposium on Research and Application of Hybrid and Composite Structures*, pp.11-11-8, 2021.11
- 5) Scherzinger, W.M. (2016). A return mapping algorithm for isotropic and anisotropic plasticity models using a line search method. *Computer Methods in Applied Mechanics and Engineering*, 317, 526-553, <https://doi.org/10.1016/j.cma.2016.11.026>.
- 6) Pech, S., Lukacevic, M., & Füssl, J. (2021). A robust multi-surface return-mapping algorithm and its implementation in Abaqus, *Finite Elements in Analysis and Design*, 190, 103531, <https://doi.org/10.1016/j.finel.2021.103531>.
- 7) MSC Software Corporation. (2019). Volume A: Theory and User Information, Chapter 5, pp. 146-151
- 8) MSC Software Corporation. (2019). Volume A: Theory and User Information, Chapter 7, pp. 818-821
- 9) Jones, R. M. (1999). *Mechanics of Composite Materials* (2nd ed.). Taylor and Francis, Inc.
- 10) Mechin, P.-Y., Keryvin, V., Grandidier, J.-C., & Glehen, D. (2019). An experimental protocol to measure the parameters affecting the compressive strength of CFRP with a fibre micro-buckling failure criterion. *Composite Structures*, 211 (1), 154-162, <https://doi.org/10.1016/j.compstruct.2018.12.026>.

(Received August 25, 2023)